

The effects of diluent molecular weight on the structure of thermally-induced phase separation membrane

B.J. Cha^c, K. Char^c, J.-J. Kim^{a,*}, S.S. Kim^b, C.K. Kim^d

^a Polymer Division, Korea Institute of Science and Technology (KIST), Cheongryang P.O. Box 131, Seoul, South Korea

^b Department of Chemical Engineering, Kyung Hee University, Yong In-Kun, Kyung Ki-Do 449-701, South Korea

^c Department of Chemical Engineering, Seoul National University, Kwan-Ak Ku, Seoul 151-742, South Korea

^d Department of Chemical Engineering, Chung-Ang University, Dong-Jak Ku, Seoul 156-756, South Korea

Received 21 July 1994; revised 10 April 1995; accepted 19 June 1995

Abstract

The effects of molecular weight of a homologous series of diluent on the droplet size of the thermally-induced phase separation membranes were investigated for the mixtures of poly(ethylene glycol) used as a diluent and nylon 12 as a matrix. All the phase diagrams obtained for different molecular weights of the diluent ranging from 200 to 600 showed the upper critical solution temperature type phase boundaries. When molecular weight of PEG was higher than 1000, nylon 12 did not form miscible blends with PEG below the thermal degradation temperature. Interaction energy density for each pair was evaluated from the phase separation temperature by the Flory–Huggins theory. The chain end group effects on the interaction energy were also considered using a binary interaction model and a Massa plot. The equilibrium domain size increased as the molecular weight of the diluent increased and then approached an asymptotic value. The increase of the average domain size with the increase of the diluent molecular weight was suppressed to a great extent for a higher content of nylon 12 in the mixture suggesting that there exist specific interactions between PEG and nylon 12.

Keywords: Diluent molecular weight; Structure; Thermally-induced phase separation; PEG; Nylon 12

1. Introduction

The thermally-induced phase separation (TIPS) process has recently been introduced to microporous membrane formation and is gaining much interest for its advantages over the conventional membrane preparation techniques. The TIPS process is applicable to a wide range of polymers since increasing temperature enhances the miscibility of polymer with diluent. Thermodynamic analysis of the TIPS process is simpler than those of the processes such as solvent casting, stretch-

ing, and track etching. The TIPS process has fewer parameters needed in controlling the microporous structure formation than the other processes. More details of the membrane formation procedure using the TIPS process were reported in many references [1–4].

The homogeneous polymer-diluent solution satisfies the phase stability conditions: the Gibbs free energy of mixing is negative and its second derivative is positive. By changing the temperature the second derivative can be converted to negative. The system reaches the upper critical solution temperature (UCST) upon cooling. When the system enters an unstable or a metastable region, it undergoes the liquid–liquid phase separation.

* Corresponding author.

In the unstable region the phase separation proceeds through spinodal decomposition followed by a coalescence or ripening process.

In the TIPS process the homogeneous polymer solution phase separates into the polymer-rich and the polymer-lean phases upon cooling. Above the critical composition of polymer, the polymer-rich phase constitutes the continuous phase, which then becomes the matrix of the membrane. The polymer-lean phase forms droplets dispersed in the continuous polymer-rich phase. In most cases the polymer-lean phase is composed of nearly pure diluent and it is easily extracted to form micropores.

Since the size control of the polymer-lean phase is directly related to the cell size control of the membrane which has been the major concern of membrane technology [5–8], understanding of the phase separation process determining the droplet size of the polymer-lean phase is crucial. It is known that the formation of droplet during the phase separation can be occurred by either coalescence or Ostwald ripening mechanism [9]. In Ostwald ripening process, the droplet size depends on interfacial tension, mobility, and the equilibrium concentrations difference between the two phases at the phase separation temperature. The interfacial tension, γ , is the most important parameter among other parameters to control the droplet size. Semiempirical relationships have been suggested for the molecular weight dependence of the interfacial tension as Eqs. (1) and (2) [10,11]:

$$\gamma^{1/4} = \gamma_{\infty}^{1/4} - k_1/M_n \quad (1)$$

$$\gamma = \gamma_{\infty} - k_2/M_n^{2/3} \quad (2)$$

where k_1 and k_2 are the semiempirical parameters, γ_{∞} is the asymptotic interfacial tension, and M_n is the number average molecular weight. It is noted from Eqs. (1) and (2) that the interfacial tension γ initially increases rapidly with the increase of the diluent molecular weight for a fixed molecular weight of polymer and then approaches an asymptotic value γ_{∞} at an infinitely high molecular weight of the diluent.

In this work blends of nylon 12 with the various kinds of poly(ethylene glycol), PEG, were prepared to examine the molecular weight effects of the PEG on the cell size of the TIPS membrane. Since the interfacial tension controlling the droplet size is known to be a function of the interaction energy and the molecular

weight [12,13], an emphasis was put on the effect of the diluent molecular weight on the domain size for a given segment–segment interaction parameter. The thermodynamic informations were obtained by the analyses at the phase boundary using the Flory–Huggins theory.

2. Experimental

2.1. Materials

Polymers used in this study were listed in Table 1. Nylon 12 was supplied by Aldrich Chemical Co. and its weight average molecular weight (M_w) is 50 500 and its polydispersity index is 4.04 according to the data provided by the supplier. The homologous series of PEG were obtained from two different sources; Junsei Chemical Co. and Polysciences. Molecular weight information of the PEGs supplied by the suppliers essentially corresponds to weight average molecular weights. The numerical value included as part of the code for these polymers indicates weight average molecular weight. All the chemicals in this work were not further purified.

2.2. Procedures

Nylon 12 and PEG were melt blended at 220°C in a round flask equipped with a mechanical stirrer. For some systems melt blending was not effective, and solvent casting method using *m*-cresol as a solvent was

Table 1
Polymers used in this study

Polymers	Molecular weight, \bar{M}_w (g/mol)	Density (g/cm ³) at 20°C	Supplier
nylon12	50 500 12 500 ^a	1.010	Aldrich
PEG200	200	1.127 ^b	Junsei
PEG400	400	1.128 ^b	Junsei
PEG600	600	1.128 ^b	Junsei
PEG1000	1000	1.101 ^c	Polysciences
PEG1540	1540	1.102 ^c	Polysciences
PEG3400	3400	1.072 ^c	Polysciences

^a \bar{M}_n

^bData from the Merck Index.

^cDensities were calculated by the group contribution method [29].

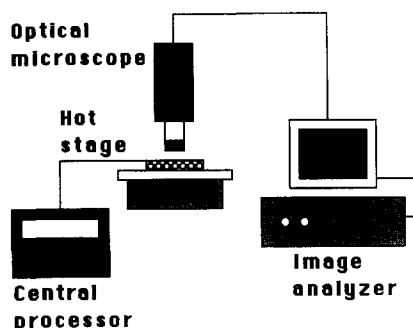


Fig. 1. Schematic diagram of the thermo-optical microscope and image analyzer system.

employed. Blends prepared by solvent casting were dried at 80°C for a week in a vacuum oven until most of the solvent evaporated. It was confirmed by thermal and optical analyses that there was no difference in the properties between the samples of the same constituents made by different methods.

The phase separation temperature on cooling was measured by light transmission technique. To explore the UCST behavior, immiscible blends were heated to temperature about 30°C above the expected phase boundary. To retain initial composition of the blend, specimens were heated in a sealed glass bottle until they become transparent, and then poured immediately onto the preheated cover slip placed on a hot stage. The edges of the bottom cover slip were sealed with teflon tape and vacuum grease to minimize PEG loss by evaporation during heating or cooling processes, and to prevent compression by the weight of the top cover slip. In order to remove the surface effects of the cover slip the distance between cover slips was set to 200 μm which is always greater than the droplet size and then the droplet in the bulk phase was observed.

For light transmission technique the quantitative intensity of light transmission through a specimen mounted on a hot stage was measured as described elsewhere [4,14,15]. Changes in transmitted light intensity were recorded as the specimens were cooled at a scanning rate of 10°C/min. The temperature at which the light intensity first changes was taken as the phase separation temperature. Videomicroscopy was also used to determine the optical phase separation temperature. Fig. 1 shows a schematic diagram of the equipment for examining the phase boundary. Changes in image of specimens mounted on a hot stages were observed as specimens were cooled at a scanning rate

10°C/min. The onset of the first diluent drop formation on cooling was taken as the phase separation temperature. Six observations for each sample were performed and averaged. The variation among each observation did not exceed $\pm 5^\circ\text{C}$. The phase separation temperatures were also determined by holding the sample for 10 min around the temperatures determined by the above methods to confirm the phase separation. The phase separation temperatures determined by the holding method deviated less than 3°C from those by 10°C/min scanning, which illustrated that cooling rate had little effects on the phase separation temperature measurement.

Average droplet sizes of the polymer-lean phase at a certain temperature were determined by a digital image analyzer (PIAS, KIT500). Specimens heated above the phase boundary were cooled to 170°C at which they underwent the phase separation, and then changes of the drop size were monitored for certain time intervals. The droplet size which did not change further after a given time period (typically 30 min.) was taken as the equilibrium droplet size. The equilibrium droplet size was also observed at a constant quench depth from the phase boundary obtained for each molecular weight of PEG. Specimens annealed to the equilibrium state at 170°C were quenched into liquid nitrogen, and PEG was extracted by acetone. For the practical application the cross section of the TIPS membrane was examined by a scanning electron microscope (SEM, Hitachi, model S-510).

3. Results and discussion

3.1. Phase diagram

Mixtures of nylon 12 and PEGs of different molecular weights ranging from 200 to 3400 were prepared for various compositions. At room temperature the samples were turbid, since it underwent the liquid–liquid phase separation and the nylon 12 crystallization. When temperature was raised to and maintained at 220°C, some of the turbid samples became clear which signifies one phase mixture. The phase separation temperatures were determined by the methods described in the experimental sections. The phase boundaries, which are the phase separation temperature plotted against the nylon 12 weight fraction, are shown in

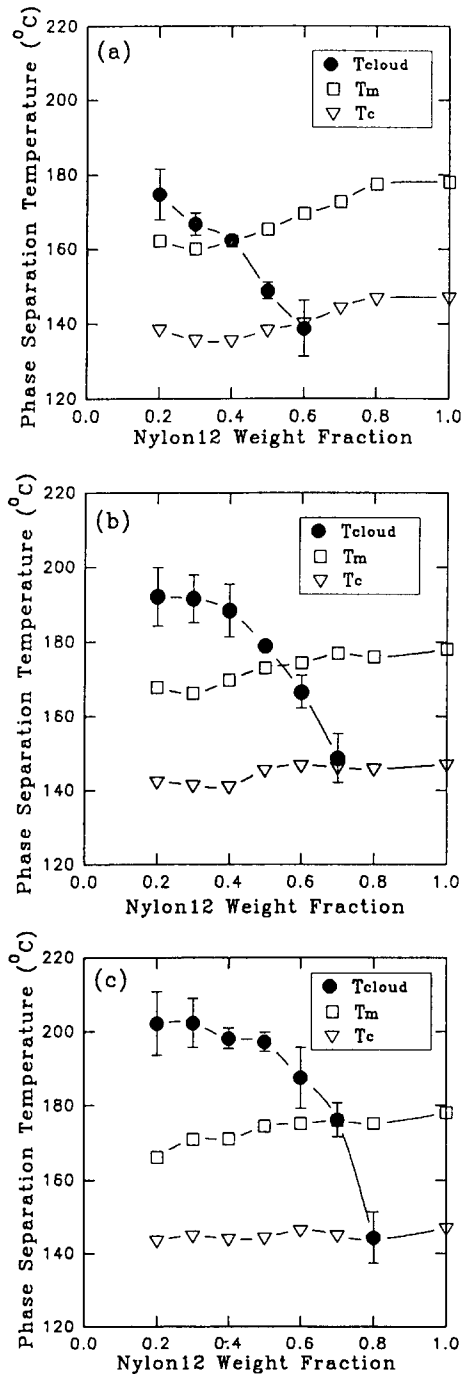


Fig. 2. Experimental phase diagrams measured under the condition of 10°C/min cooling rate: (a) nylon 12/PEG 200 blend; (b) nylon 12/PEG 400 blend; (c) nylon 12/PEG 600 blend.

Fig. 2 for three different molecular weights of PEG. All three phase diagrams showed the UCST type phase

behavior typical for the mixtures of the polymer and the low molecular weight substance. As the molecular weight of PEG increased the phase boundary was shifted to the higher temperature due to the decrease of the combinatorial entropy. When the molecular weight of PEG is greater than 1000, mixtures were not homogenized below the thermal degradation temperatures of the samples. Since nylon 12 is a semicrystalline polymer the liquid–liquid phase separation curve is expected to be intersected by a crystallization line, the intersection of which was called a monotectic point.

When we select a high value of nylon 12 weight fraction such that the crystallization line is above the liquid–liquid phase separation curve the solid–liquid phase separation then occurs first upon cooling from one phase region. It was also noted that the monotectic composition of nylon 12 increased with the increase of the molecular weight of the diluent. The crystallization line inside the liquid–liquid phase envelope is almost horizontal as shown in Fig. 2, which is the characteristic of the liquid–liquid phase separation. For nylon 12 weight fractions less than 0.2 experimental determination of the phase boundary was difficult due to the phase inversion. This region of nylon 12 weight fraction is irrelevant to the real membrane application.

In order to better understand the phase behavior of the nylon 12 and PEG mixtures, the Flory–Huggins theory [16,17] was employed to obtain the interaction energy density between nylon 12 and PEG. The Flory–Huggins theory which ignores the compressibility of pure components and their mixtures is only an approximation of the real system behaviors. However, quantitative information on interaction obtained by this theory is still an important element in understanding the thermodynamic phase behavior of the mixtures. Since nylon 12 and PEG systems have polar interactions, the analysis using generalized equation-of-state theories which incorporate the specific interaction [18,19] is required among existing equation-of-state theories [20–23]. This type of approach is beyond the scope of this paper. The Gibbs free energy change of mixing per unit volume, EMBED Equation, is expressed as sum of combinatorial entropy and non-combinatorial energetic terms as follows [16,17]:

$$\Delta g_m = RT \left[\frac{\phi_1 \ln \phi_1}{\bar{V}_1} + \frac{\phi_2 \ln \phi_2}{\bar{V}_2} \right] + B \phi_1 \phi_2 \quad (3)$$

Table 2
Molar volume as a function of temperature^a for each polymer

Polymer	Molar volume ($\bar{M}_w/\text{density}$)
Nylon 12	$50\,500/(1.0698-5.670 \times 10^{-4}T)^b$
PEG 200	$200/(1.1183-7.526 \times 10^{-4}T)^c$
PEG 400	$400/(1.1078-7.926 \times 10^{-4}T)^c$
PEG 600	$600/(1.1143-7.695 \times 10^{-4}T)^c$

^a T is in °C.

^bDensity was calculated by the group contribution method [29].

^cDensities and their temperature dependencies were measured using a dilatometer in our laboratory.

Note that the molar volume listed in Table 2 is equal to molecular weight divided by density. By assuming that the measured phase separation temperature corresponds to the binodal points, the interaction energy can be extracted from the condition of equilibrium.

$$\Delta\mu_1^\alpha = \Delta\mu_1^\beta, \quad \Delta\mu_2^\alpha = \Delta\mu_2^\beta \quad (4)$$

Where the α and β denotes the different phases and $\Delta\mu_1$ is given by

$$\Delta\mu_1 = RT[\ln \phi_1 + (1 - \tilde{V}_1/\tilde{V}_2)\phi_2 + B\phi_2^2] \quad (5)$$

The interaction energy densities between nylon 12 and PEG estimated at two different compositions by solving Eq. (4) simultaneously are listed in Table 3. The interaction energies obtained by the Flory–Huggins theory were not the same for the various blends. As mentioned elsewhere [15], though these differences could come from several sources, end groups might be the dominant factor in this mixture. Interaction energy in this system can be strongly influenced by the hydroxyl end groups of PEG. Hata and Kase-mura [24] demonstrated that the surface tension and density of poly (ethylene glycol) and poly (propylene glycol) drastically changes as the end group is varied from a hydroxyl group to a methyl group. The surface tension of hydroxyl terminated PEG, which is the same type of PEG used in this study, measured near room temperature has been found to be almost independent of molecular weight [25,26]. This effect has been attributed to the cluster formation originating from hydrogen bonding among hydroxyl terminated groups and ether oxygen in the main chain leading to the behavior equivalent to infinite molecular weight. The specific hydrogen bonding effect of the hydroxyl terminated PEG is expected to decrease at an elevated temperature.

In order to estimate the interaction energy density between ethylene oxide and nylon 12 segments two different approaches were taken. One is to use the binary interaction model [27] in which a PEG chain is considered as a copolymer consisting of ethylene oxide and hydroxyl segments:

$$B = B_{13}\phi_1 + B_{23}\phi_2 - B_{12}\phi_1\phi_2 \quad (6)$$

where subscript 1 denotes the hydroxyl end groups, 2 the ethylene oxide and 3 the nylon 12 segments. Since we have three interaction values for the diluent PEG of molecular weights 200, 400 and 600, the B_{13} , B_{23} , and B_{12} , can be determined by solving simultaneous linear algebraic equations. The interaction energy density between ethylene oxide and nylon 12 segments (B_{23}) was estimated to be 0.18 cal/cm^3 . The other interaction energies deduced by this analysis are $B_{13} = 22.6 \text{ cal/cm}^3$ and $B_{12} = 1.1 \text{ cal/cm}^3$. The extremely high value of B_{13} seemed to be unreasonable suggesting the possible self-association effect of PEG which was not considered in this model. The other method was to extrapolate the experimentally determined interaction energy to infinite molecular weight of PEG where the possible end functional group effects are negligible. Fig. 3 shows the Massa plot [28] in which experimentally determined interaction energy density is plotted against the sum of inverse of the molecular weight of each component. All the interaction energy density values experimentally determined for different molecular weights of PEG fell nicely on a straight line as shown in Fig. 3. The interaction energy density value extrapolated to infinite molecular weight from the Massa plot is 0.098 cal/cm^3 . There is a difference in interaction energy density determined from the two methods mentioned. We believe that the latter value is more reasonable since the former case does not include the self-association appropriately.

Table 3
Flory–Huggins interaction energy densities (cal/cm^3)

Interacting pair	B ($\phi_{\text{PEG}}=0.8$)	B ($\phi_{\text{PEG}}=0.5$)
Nylon 12/PEG 200	2.6252	3.3112
Nylon 12/PEG 400	1.3581	1.7082
Nylon 12/PEG 600	0.9514	1.1950

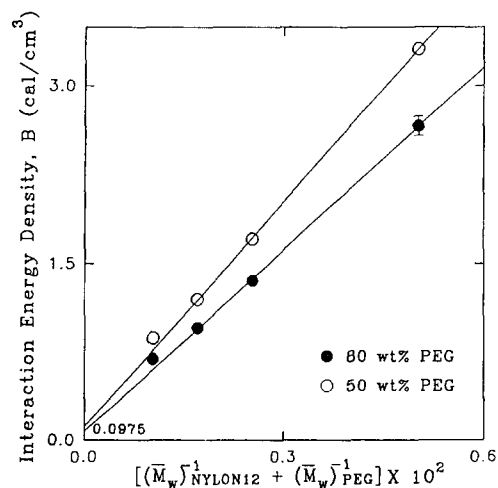
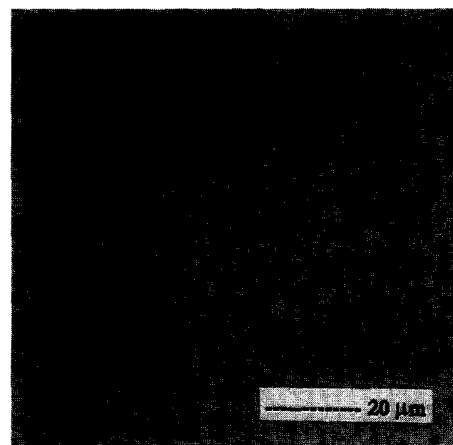


Fig. 3. The Massa plot showing the change of interaction energy densities for blends of nylon 12 with PEG having various molecular weights.

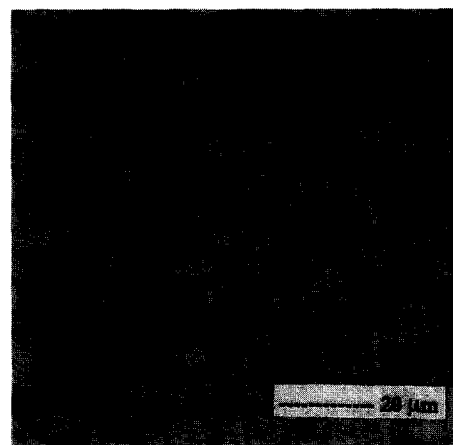
3.2. Molecular weight dependence of domain size

The growth of PEG rich domain size was observed on a hot stage with an optical microscope for the mixtures of PEG and nylon 12 (80/20 by weight) as shown in Fig. 4 for a PEG molecular weight of 200, 400 and 600, respectively. These pictures were obtained with the image analysis system connected to an optical microscope for samples maintained isothermally at 170°C after deep quenching of 20°C/min from homogeneous mixtures. The calculated number average domain size from the photographs as a function of time was shown in Fig. 5 for different molecular weights of PEG (200, 400 and 600) as well as for different weight fractions of PEG. Since the blend containing 50 wt% PEG 200 was not phase separated at 170°C as shown in Fig. 2, the domain size was not reported in Fig. 5. In case of PEG weight fraction of 0.8 the PEG rich domains initially grew and then leveled off at a fixed domain size after a certain time period. Domain size of PEG fraction of 0.5 was slightly increased with time.

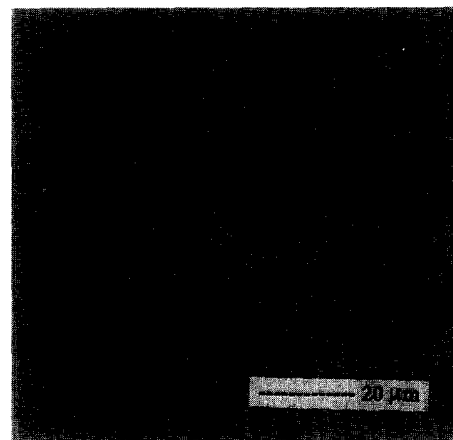
The final domain size observed in this work might not reflect equilibrium domain size because of slow kinetics of phase separation. To explore this issue, some mixtures containing 50 wt% and 80 wt% of PEG were annealed for one day at 170°C. Changes in domain size was not observed after about 30 min annealing. In our opinion, the final domain size reported here reflected



2 min



4 min

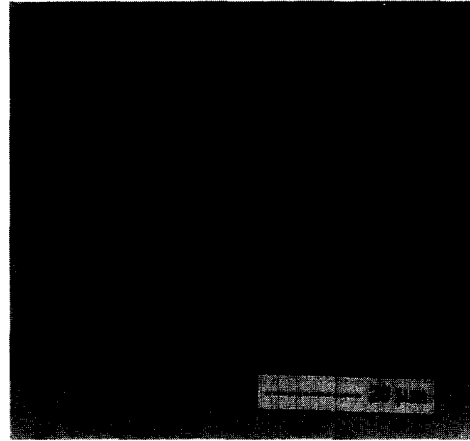


20 min

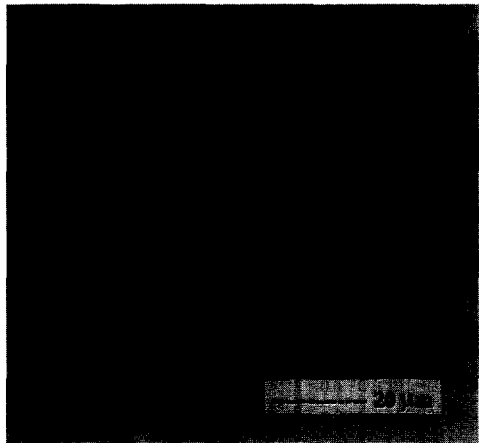
(a) nylon12/PEG200 = 20/80



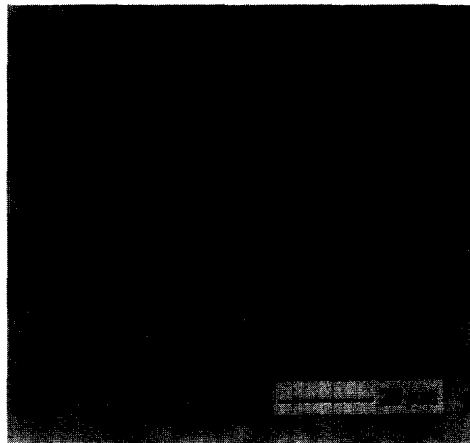
2 min



3 min



5 min

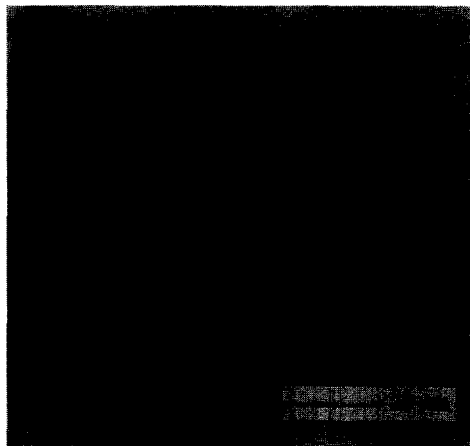


10 min



30 min

(b) nylon12/PEG400 = 20/80



40 min

(c) nylon12/PEG600 = 20/80

Fig. 4. Time dependent phase separation behavior for 80 wt% PEG blends annealed at 170°C after 20°C/min cooling rate ($\times 800$): (a) nylon 12/PEG 200 (20/80); (b) nylon 12/PEG 400 (20/80); (c) nylon 12/PEG 600 (20/80).

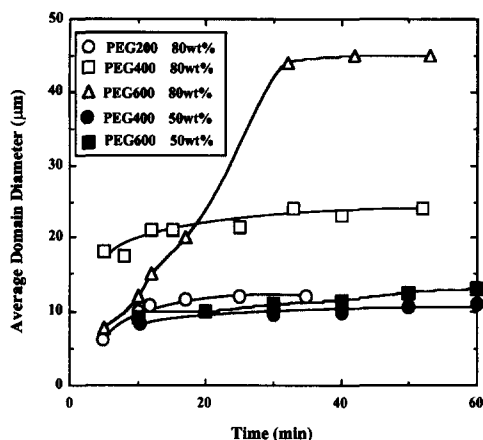


Fig. 5. Change of phase separated domain size with time obtained from image analyzer system. Blends were maintained at 170°C for 1 h after 20°C/min cooling rate.

the equilibrium domain size. In case of PEG weight fraction of 0.8 the equilibrium domain size for PEG 600 was much larger than that for PEGs of 200 and 400, while the equilibrium domain size for PEG 200 was smaller than that for PEG 400. In contrast to the PEG weight fraction of 0.8, the domain size for PEG weight fraction of 0.5 remained relatively at a low value.

Fig. 6 shows the number average equilibrium domain size estimated from photographs under image analyzer as a function of molecular weight of diluent PEG for two different weight fractions of PEG. Note that the homogeneous melt blends were not formed until the sample reached the thermal degradation temperature, when the molecular weight of PEG was greater than 1000. Thus, the phase separated blends at 220°C were quenched to 170°C and their equilibrium domain sizes were measured. The increase of domain size with increasing PEG molecular weight was more evident for PEG fraction of 0.8 than for PEG fraction of 0.5. In case of PEG weight fraction of 0.8 the pore size varies from 10 μ to 45 μ as the molecular weight of PEG increased from 200 to 600 and then leveled off when molecular weight of PEG was higher than 600. The effect of the PEG molecular weight on the TIPS membrane structure was less pronounced for the case of 0.5 PEG weight fraction than that of 0.8 PEG weight fraction. Exact explanations for composition dependence of diluent domain size were not given at this point. An infrared spectroscopy study is being conducted to examine this fact.

From the above results in Fig. 6 it is believed that there exist specific interactions between ether oxygen or hydroxyl end group of PEG and amide functional group from nylon 12. Even though the interaction energy density between ethylene oxide and nylon 12 segments calculated from the phase diagram was slightly repulsive ($B \sim 0.1$ cal/cm³) there seemed to be favorable interaction such as hydrogen bonding between the ether oxygen and the amide functional groups since repeat unit of the nylon 12 contains additional 11 methyl groups. As the nylon content is increased the interaction between ether oxygen and amide functional group was more probable yielding small domain size with less pronounced molecular weight effect of diluent PEG. In addition, the self-association of PEG was hindered by blending with nylon 12. The surface tension of hydroxyl terminated PEG is known to be almost independent of its molecular weight due to its self-association behavior [25,26]. If this is the case the domain size should remain constant even when the molecular weight of diluent changed. As soon as PEG chains were in contact with nylon 12 it seemed that the self-association of PEGs was hindered by specific interactions of ether oxygen and/or hydroxyl terminal groups of PEG with amide groups from nylon 12 showing molecular weight dependency of pore size. It is necessary to examine chain end effects by using methyl terminated PEG's for which it is known that the hydrogen bonding effect among end groups is absent [26]. It will be the topic of our forth-

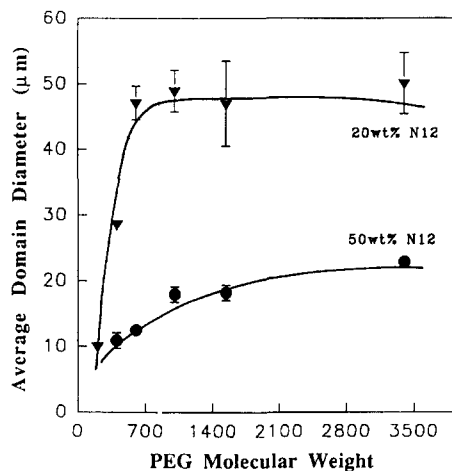


Fig. 6. Change of equilibrium domain size with molecular weight of PEG for 0.8 and 0.5 weight fractions determined from the image analyzer.

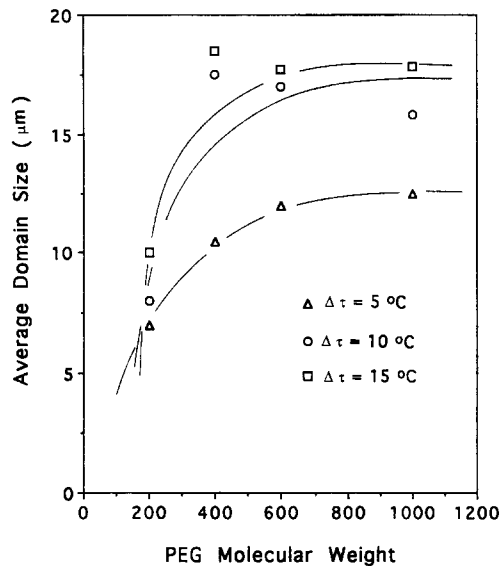


Fig. 7. Number average domain size as a function of PEG molecular weight for different quench depths for the binary mixture of nylon 12 and PEG (20/80 by weight).

coming paper. Consequently, the average domain size initially increased for PEG molecular weight ranging from 200 to 600 and the domain size then leveled off. This trend qualitatively corresponded to the prediction given in Eqs. (1) and (2).

Since the phase separations for nylon 12/PEG binary mixture have been carried out so far at a fixed temperature (170°C), the material parameters such as viscosity, molecular weight of PEG, interfacial tension, and thermodynamic driving force such as quench depth ($\Delta\tau$) are interrelated. In order to single out the effect of thermodynamic driving force, the average equilibrium domain size of the phase separated PEG rich phase was measured as a function of diluent molecular weight for different quench depth ($\Delta\tau = 5, 10, 15^\circ\text{C}$) as shown in Fig. 7. It was first noted that the effect of PEG molecular weight on the average domain size was much reduced at constant quench depth. As the quench depth increased the average domain size increased as expected. It should be noted that the crystallization was not observed for all the samples examined in this work.

The microporous TIPS membranes structure was generated by extracting the diluent rich phase. Fig. 8 showed scanning electron microscope (SEM) images of the cell structures obtained for mixtures of 0.8 PEG weight fraction for three different molecular weights of PEG. The volume contraction of the sample was



Fig. 8. Scanning electron microphotographs of the cross section of a membrane prepared from blends of nylon 12 with PEG having various molecular weights quenched in liquid nitrogen after being annealed at 170°C for 1 h and extracted with acetone ($\times 2000$): (a) nylon 12/PEG 200 (20/80); (b) nylon 12/PEG 400 (20/80); (c) nylon 12/PEG 600 (20/80).

induced by the crystallization of nylon 12 and losing diluent in the nylon rich phase during extraction and drying, and thus obtained cell size also decreased. However, a qualitative relationship exists between the domain size on an optical microscope and the cell size of the membranes. As predicted from the domain growth observed with optical microscope the cell size was also larger as molecular weight of PEG increased. It is clear that the cell size required for specific membrane application can be regulated by changing the molecular weight of homologous series of PEG.

4. Conclusions

The effects of diluent molecular weight on the pore size of the TIPS membrane were investigated. The phase diagrams were experimentally determined for the mixtures of PEG used as a diluent and nylon 12 as a polymer matrix. All the phase diagrams obtained showed the UCST behavior and the solid–liquid phase separation as well as the liquid–liquid phase separation was determined. As the molecular weight of PEG increased the two phase region was expanded due to the decrease of the combinatorial entropy. The interaction energy densities were calculated from the phase diagrams by using the Flory–Huggins theory and were dependent upon the molecular weight of PEG as well as the PEG content in the mixture suggesting that the effect of hydroxyl end groups of PEG was quite important in this system. Mass plot was employed to take into account the end group effect and yielded a reasonable interaction energy density value between the ethylene oxide and nylon segments compared with the binary interaction model.

The equilibrium domain size was determined from studying the time dependent phase separation behavior by using an image analyzer connected to an optical microscope. It was noted that the equilibrium domain size increased as the molecular weight of PEG increased and the behavior was analogous to the increase in interfacial tension as a function of molecular weight. It was also noted that domain size increase was less pronounced for the case of lower content of PEG in the mixture suggesting that there exists specific interactions such as hydrogen bonding between PEG and nylon 12.

Acknowledgements

The authors gratefully acknowledge the financial support from KIST and the Kolon Group Owoon Foundation.

References

- [1] A.J. Castro, Method for making microporous products, U.S. Pat., 4,247,498, assigned to Akzona Inc., 1981.
- [2] D.R. Lloyd, J.W. Barlow and K.E. Kinzer, Microporous membrane formation via thermally-induced phase separation, *AIChE Symp. Ser.*, 261 (84) (1989) 28.
- [3] D.R. Lloyd, S.S. Kim and K.E. Kinzer, Microporous membrane formation via thermally-induced phase separation. II. Liquid–liquid phase separation, *J. Membrane Sci.*, 64 (1991) 1.
- [4] S.S. Kim, Thermodynamics and structure study of tips membrane, Ph.D. Dissertation, The University of Texas at Austin, August, 1990.
- [5] R.E. Kesting, *Synthetic Polymeric Membrane*, Wiley, NY, 1985.
- [6] P.M. Subramanian, Permeability barriers by controlled morphology of polymer blends, *Polym. Eng. Sci.*, 25 (1985) 483.
- [7] P.M. Subramanian and M. Mehra, Lamellar morphology in polymer blends: structure and properties, *Polym. Eng. Sci.*, 27 (1987) 663.
- [8] M.R. Kamel, I.A. Jinnah and L.A. Utracki, Permeability of oxygen and water vapor through polyethylene/polyamide films, *Polym. Eng. Sci.*, 24 (1984) 1337.
- [9] T. Hashimoto, Dynamics in spinodal decomposition of polymer mixtures, in *Phase Transition*, Vol. 12, 1988, p. 47.
- [10] S.J. Wu, Interfacial and surface tensions of polymers, *Macromol. Sci., Rev. Macromol. Chem.*, C10 (1974) 1.
- [11] D.G. LeGrand and G.L. Gains, The molecular weight dependence of polymer surface tension, *J. Colloid Interface Sci.*, 31 (1969) 162.
- [12] E. Helfand and A.M. Sapse, Theory of interface between immiscible polymers II, *J. Chem. Phys.*, 62 (1975) 1327.
- [13] E. Helfand and Y. Tagami, Theory of unsymmetric polymer–polymer interfaces, *J. Chem. Phys.*, 56 (1972) 3592.
- [14] C.K. Kim and D.R. Paul, Interaction parameters for blends containing polycarbonates: 1. TMPC/PS, *Polymer*, 33 (1992) 1630.
- [15] T.A. Callaghan and D.R. Paul, Interaction energies for blends of pmma, ps, and poly(methyl methacrylate), by the critical molecular weight method, *Macromolecules*, 26 (1993) 2439.
- [16] P.J. Flory, Thermodynamics of high polymer solutions, *J. Chem. Phys.*, 10 (1942) 51.
- [17] M.L. Huggins, Solutions of long chain compounds, *J. Chem. Phys.*, 9 (1941) 440.
- [18] I.C. Sanchez and R.H. Lancomb, Statistical thermodynamics of polymer solutions, *Macromolecules*, 11 (1978) 1145.
- [19] I.C. Sanchez, An elementary equation of state for polymer liquids, *Polym. Lett. Ed.*, 15 (1977) 71.

- [20] I.C. Sanchez and R.H. Lancomb, Statistical thermodynamics of fluid mixtures, *J. Phys. Chem.*, 80 (1976) 2352.
- [21] I.C. Sanchez and A.C. Balazs, Generalization of the lattice fluid model for specific interactions, *Macromolecules*, 22 (1989) 2325.
- [22] Y.S. Lipatov, A.E. Nestenov and T.D. Ignatova, Some peculiarities of thermodynamic behavior oligomeric mixtures with specific interactions between components, *Eur. Polym. J.*, 15 (1979) 775.
- [23] D.R. Paul, J.W. Barlow and H. Keskkular, Polymer blends, in *Encyclopedia of Polymer Science and Engineering*, Vol. 12, Wiley, NY, 1988, p. 399.
- [24] T. Hata and T. Kasemura, Surface and interfacial tensions of polymer melts and solutions, *Polym. Sci. Technol.*, 12A (1980) 15.
- [25] B.B. Sauer and G.T. Dee, Molecular weight and temperature dependence of polymer surface tension: comparison of experiment with theory, *Macromolecules*, 24 (1991) 2124.
- [26] A.K. Rastogi and L.E. St. Pierre, Interfacial phenomena in macromolecular systems. V. The surface free energies and surface entropies of polyethylene glycols and polypropylene glycols, *J. Colloid Interface Sci.*, 35 (1971) 16.
- [27] D.R. Paul and J.W. Barlow, A binary interaction model for miscibility of copolymers in blends, *Polymer*, 25 (1984) 487.
- [28] D.J. Massa, Physical properties of blends of polystyrene with poly(methyl methacrylate) and styrene/(methyl methacrylate) copolymers, *Adv. Chem. Ser.*, 176 (1979) 433..
- [29] D.W. van Krevelen, *Properties of Polymers*, Elsevier, NY, 1990.